GEOPHYSICAL RESEARCH LETTERS, VOL. 29, NO. 17, 1836, doi:10.1029/2002GL015357, 2002

Detection of aerosol types over the East China Sea near Japan from four-channel satellite data

Akiko Higurashi
National Institute for Environmental Studies, Ibaraki, Japan

Teruyuki Nakajima
Center for Climate System Research Center, The University of Tokyo, Tokyo, Japan

Received 19 April 2002; revised 19 July 2002; accepted 13 August 2002; published 11 September 2002.

[1] Aerosol-type detection from satellite remote sensing is difficult but an important challenge for improving the estimation of aerosol radiative forcing. In this paper, we have classified aerosols into four major aerosol types, that is, soil dust, carbonaceous, sulfate and sea salt aerosols using SeaWiFS four-channel data. The retrieved results show that the East China Sea region was loaded with different aerosols in a highly mixed condition. We also succeeded in classifying the volcanic plume from Mt. Oyama located on Miyakejima Island as sulfate aerosols. *INDEX TERMS:* 0305 Atmospheric Composition and Structure: Aerosols and particles (0345, 4801); 0345 Atmospheric Composition and Structure: Pollution—urban and regional (0305); 0370 Atmospheric Composition and Structure: Volcanic effects (8409); 1610 Global Change: Atmosphere (0315, 0325); 1640 Global Change: Remote sensing. **Citation:** Higurashi, A., and T. Nakajima, Detection of aerosol types over the East China Sea near Japan from four-channel satellite data, *Geophys. Res. Lett.*, *29*(17), 1836, doi:10.1029/2002GL015357, 2002.

1. Introduction

[2] Aerosols directly and indirectly affect the Earth's climate, since they scatter and absorb radiation and also alter the cloud microphysical properties. Despite the significance of such aerosol climate effects, the accurate evaluation of the aerosol radiative forcing have not yet been clarified due to our poor knowledge of aerosol properties and the mechanism of aerosol-cloud interaction on a global scale [*IPCC*, 2001]. Aerosol type is one of the important parameters for the forcing evaluation, since the aerosol climate effects considerably differ from one type to another. The most important aerosol types are soil dust, carbonaceous, sulfate, and sea salt aerosols. Their representative particle size and radiation absorptivity are quite different. Soil dust aerosol particles, for example, are large in size and significantly absorb shortwave radiation, while sulfate aerosol particles are small in size and are non-absorbing. Carbonaceous aerosols are more complicated in their chemical and optical properties, but they are commonly recognized as a strongly absorbing aerosol with the inclusion of soot particles.

0094-8276/02/2002GL015357$05.00

[3] This difficult situation started being eased by the recent rapid progress in the satellite remote sensing techniques of aerosols. A two-channel algorithm retrieves the aerosol optical thickness and Ångström exponent as a particle size index [*Nakajima and Higurashi*, 1998; *Higurashi and Nakajima*, 1999; *Mishchenko et al.*, 1999; *Higurashi et al.*, 2000]. POLDER made it possible to retrieve aerosol distributions over land using polarized radiance [*Deuzé et al.*, 2001]. The UV algorithm of *Herman et al.* [1997] was successful in using TOMS UV radiances to detect absorbing aerosols, such as soil dust and biomass burning aerosols, which strongly absorb UV and blue radiation, as also shown by *Dubovik et al.* [2000] with AERONET data analysis.

[4] In this paper, we propose a new algorithm of an aerosol type classification combining the two-channel method and the UV method.

2. Method

[5] The proposed four-channel algorithm is roughly divided into two steps. The first step is almost the same as that of the two-channel algorithm of *Higurashi and Nakajima* [1999] to derive the aerosol optical thickness and effective radius. The new algorithm assumes two aerosol optical models, that is, absorbing and non-absorbing aerosol models for the inversion process to obtain a set of aerosol optical thickness and Ångström exponent values for each aerosol model. We use spectral radiances in channels 6 and 8 of the SeaWiFS satellite-borne imager with the center wavelengths at 670 and 865 nm, respectively. Here we define the Ångström exponent as the slope of a log-linear regression line to the spectral optical thickness calculated at wavelengths of 368, 500, 675, 862, and 1050 nm.

[6] In the second step of our algorithm, we test the blue radiation absorptivity of aerosol particles in the SeaWiFS channels 1 and 2, of which the center wavelengths are 412 and 443 nm, respectively. The difference in the apparent aerosol reflectance between channels 1 and 2 for the absorbing model is smaller than that for the non-absorbing model as confirmed by several numerical simulations, as understood by the following approximated relation for the difference in reflectances at the two wavelengths:

$$\Delta\rho = \rho_{412} - \rho_{443} \approx \pi\left(\omega_{412}\tau_{a,412} - \omega_{443}\tau_{a,443}\right)P(\Theta)/\mu\mu_0, \quad (1)$$

where ω, τ_a, $P(\Theta)$, μ, and μ_0 are, respectively, the aerosol single scattering albedo, optical thickness, scattering phase

Table 1. Wavelength-Averaged Values of the Refractive Index in SeaWiFS Channels

	Absorbing model				Non-absorbing model			
Channel No.	1	2	6	8	1	2	6	8
Real part	1.5	1.5	1.5	1.5	1.438	1.434	1.428	1.425
Imaginary part	0.012	0.008	0.005	0.005	9.99E-9	9.97E-9	1.72E-8	1.95E-7

function at the scattering angle of Θ, cosine of the nadir angle of the emergent ray, and cosine of the solar zenith angle. We utilize in Equation (1) the fact that the normalized scattering phase function has a similar value at wavelengths closely located to each other. In the second step, therefore, we can select a suitable aerosol optical model by comparing the difference in the blue channel radiances observed and calculated with the aerosol optical thickness and Ångström exponent retrieved in the first step. The refractive index for each model is referenced to sulfate of *WCP-55* [1983] for the non-absorbing model and to *Sokolik et al.* [1993] for the absorbing model. The wavelength-averaged values of the refractive index for SeaWiFS channels are shown in Table 1. The size distribution is a bimodal log-normal function as same as that used by *Higurashi and Nakajima* [1999]. We have classified the aerosols into the following four types based on the retrieved Ångström exponent and blue-spectral radiative absorptivity. We divided the aerosols into large particles and small particles according to the Ångström exponent value assuming a boundary value of 0.8. The resulting classified aerosol types are the 'Soil dust aerosol' as the absorbing aerosol with a small Ångström exponent, 'Carbonaceous aerosol' as the absorbing aerosol with a large Ångström exponent, 'Sulfate aerosol' as the non-absorbing one with a large Ångström exponent, and 'Sea salt aerosol' as the non-absorbing one with a small Ångström exponent. Although we label these four types as 'Soil dust', 'Carbonaceous', 'Sulfate', and 'Sea salt', these types should be regarded as optically equivalent aerosol types mimicking the realistic aerosols, which should have more complicated optical properties and chemical compositions.

[7] The validation with ground-based measurements is important for the satellite remote sensing of aerosols, since aerosol signals are small and sensitive to sensor degradation. Figures 1a and 1b are plots of satellite-derived versus ground-based aerosol optical thickness data at the wavelength of 500 nm and the Ångström exponent. The ground-based data were derived from a PREDE skyradiometer at the Miyakojima Island site (24.733°N, 125.317°E), as one of the National Space Development Agency of Japan (NASDA) validation sites called SKYNET, sampled within 30 minutes before and after the satellite pass, and the SeaWiFS-derived data are selected within 0.5 degrees from the ground site. We also plot the results from the two-channel algorithm assuming the bi-modal size distribution and the absorbing or non-absorbing model. Both parameters derived by the four-channel algorithm show better agreement with the ground-based values, suggesting that the correlation between the retrieved and observed values is improved by the introduction of model-selection. The correlation coefficient of the optical thickness plots is calculated as 0.93 for the four channel result, whereas 0.73 and 0.79 for the two channel results with the absorbing and non-absorpbing models, respectively. The correlation coefficient values of the Ångström exponent plot are respectively 0.70, 0.72, and 0.72, indicating the nonsignificance of the models.

3. Aerosol Characteristics Over the East China Sea Near Japan

[8] We have analyzed the SeaWiFS data acquired in the Asian Atmospheric Particle Environmental Change Studies (APEX), a project of the Japan Science and Technology Corporation (JST), conducted together with the International Asian Aerosol Characterization Experiment (ACE-Asia) in the spring of 2001 in a zone of the East China Sea from 15°N to 55°N and from 110°E to 160°E. Figure 2a shows a near-real color image of SeaWiFS on April 14, which is synthesized from channels 1, 5 and 6 overlaid with a weather map. Chinese soil dust aerosol is called 'Kosa' in Japanese meaning the yellow sand, as clearly indicated by the yellowish colored plume in the figure. On this day, it was transported over Japan by a low-pressure system traveling eastward.

[9] Figures 2b–2d show the aerosol optical thickness at 500 nm, Ångström exponent, and absorptivity, while the aerosol type is shown in Figure 2e. In the Asian dust plume area, the optical thickness was greater than 1, and Ångström exponent was as small as 0.6. Since the algorithm judged this aerosol plume as absorbing aerosols, this plume was successfully classified as 'Soil dust aerosol' and consistent with the visual judgment in Figure 2a. The area adjacent to the coast of the continent was found to be covered by aerosols with large Ångström exponent values indicating the effect of a polluted air mass from the continent. This area is classified as 'Carbonaceous aerosol' in our analysis. This result suggests that soil dust aerosols and air pollution aerosols were highly mixed in this region on this day. In this regard, it is interesting to find that the Ångström exponent

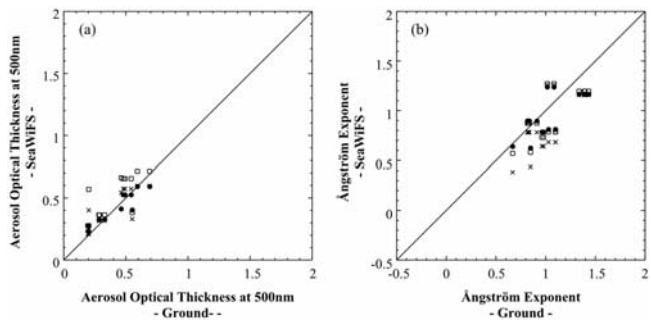

Figure 1. The correlation between satellite-derived and ground-based aerosol optical thicknesses (a) and Ångström exponents (b). The satellite-derived results from the four-channel algorithm (solid circle), and from the two-channel algorithm assume the absorbing model (square) and the non-absorbing model (cross).

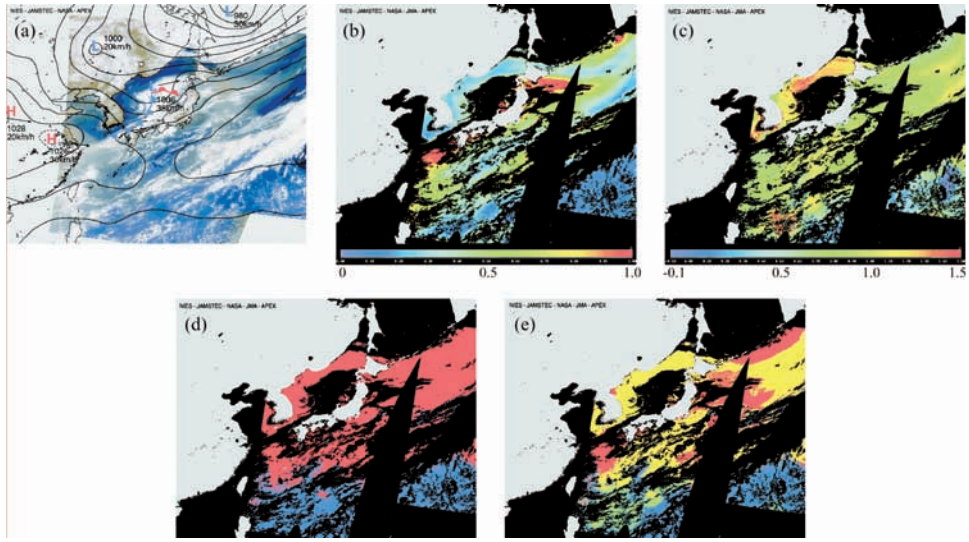

Figure 2. A near true-color image synthesized from SeaWiFS spectral radiances (a), retrieved aerosol optical thickness at 500 nm (b) Ångström exponent (c) absorptivity (d) and aerosol type (e) on April 14, 2001. In panel (d) the red and blue colors indicate the absorbing and non-absorbing aerosols, respectively. The aerosol types shown in panel (e) are soil dust (red), carbonaceous (yellow), sulfate (green), and sea salt (blue) aerosols.

of the dust plume of 0.6 is not as small as 0.3 to 0.4 of the Saharan dust plume found by *Deuzé et al.* [1999] and *Higurashi et al.* [2000]. This phenomenon can be understood as the dust plume was mixed with air pollution aerosols to decrease the effective particle size of the mixed polydispersion. As an independent method of detecting dust and carbonaceous aerosols, the TOMS aerosol index (data are available from the world wide web server for the ACE-Asia mission at http://hyperion.gsfc.nasa.gov/Missions/ACEASIA/satellite/index.html.) was investigated in this region, but there was no significant TOMS signal on this day, different from our analysis. One of the reasons for the failing of some aerosol plume signals is that the TOMS detection method is highly dependent on the optical thickness and the height of the aerosol plume. This fact suggests some advantage of our method over the TOMS method for detecting absorbing aerosols with higher sensitivity, finer field of view, and less effect from Rayleigh scattering.

[10] In the open sea area, the algorithm successfully classified the aerosols as 'Sea salt' with the aerosol optical thickness less than 0.1, and with a small Ångström exponent. It should be noted that the sulfate aerosol type was detected only in a small area of Figure 2e, while the carbonaceous aerosol type covered most of the region affected by the outflow from the continent. A numerical test has shown that our algorithm tends to choose the carbonaceous aerosol when the contribution of carbonaceous aerosols in the total aerosol optical thickness is greater than about 30%, although the critical value depends on the detailed condition of the retrieval. Therefore, our result means that the carbonaceous aerosol contribution is dominant in this region. This observation is consistent with the recent model simulations suggesting that the optical thickness of the carbonaceous aerosols is as large as that of the sulfate aerosols in this region [*Takemura et al.*, 2000].

[11] One more interesting result concerning the aerosol classification is shown in Figures 3a and 3b, which are a near-true color image of SeaWiFS and the map of the retrieved aerosol type around the Izu Islands on May 4, 2001. Volcanic plumes are clearly seen from Mt. Oyama in Miyakejima Island (34.079°N, 139.529°E) and these plumes are suitably classified as sulfate aerosols. This result is consistent with the report by the JMA (Japan Meteorological Agency), which tells that Mt. Oyama discharged 2×10^4 tons of SO_2 every day in the period of March to May 2001 (the reports about this are available from the world wide web server of JMA at http://www.kishou.go.jp/press/miyake/index.html). There have been few reports of the direct measurement of volcanic plumes from satellites. *Bluth et al.* [1992] used TOMS data to detect SO_2 clouds emitted from the Mt. Pinatubo eruption in 1991. The sensitivity of this method is not very high such that a narrow plume near the volcano cannot be detected. There are reports using the thermal split window channels of AVHRR [*Prata*, 1989; *Wen and Rose*, 1994; *Kinoshita et al.*, 1998]. This method has the advantage of high spatial resolution detection of narrow plumes with widths of several kilometers both under day and night conditions. The sign of the brightness temperature difference is opposite

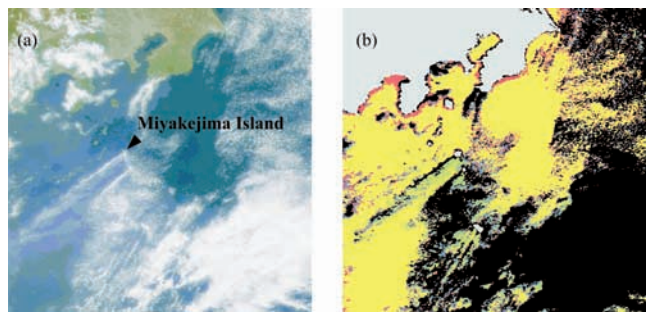

Figure 3. A near-true color image of SeaWiFS (a) and retrieved aerosol type (b) on May 4, 2001 from 32°N to 36°N and from 138°E to 142°E. Color codes are the same as that in Figure 2e.

from that of high-level cirrus clouds, because of the different wavelength dependence of the single scattering albedo of volcano ash particles from that of ice particles. This algorithm is, however, affected by the vertical temperature profile, thus making it difficult to be applied to a quantitative estimate of the volume of the volcanic ash. On the other hand, our method uses the difference in the optical properties of aerosols in the blue to red spectral region, and can provide high spatial resolution information independent from the thermal method. Especially, it is not difficult to estimate the mass of the volcanic aerosols, M, by the relation:

$$M = \frac{4\rho r_e \tau_a WV}{3Q_e}, \quad (2)$$

where ρ, τ_a, Q_e, W, and V are the aerosol density, optical thickness, extinction efficiency factor for particle size r_e, width of the smoke plume, and wind velocity, respectively. We analyzed 12 volcanic plumes identified in April and May, obtaining the plume parameters from satellite images and the retrieved results from the four-channel method. Assuming an extinction efficiency factor of 3.01 for a typical effective radius of 0.5 μm [*Lacis and Mishchenko*, 1995] and the density of volcanic aerosol of 2.5 g/cm^3, the aerosol mass was roughly estimated as 4365 tons/day. This value means a conversion rate of about 23% of the total SO_2 emission if we believe the value of 2×10^4 tons/day reported by JMA. This conversion rate is considered to be reasonable, because recent aerosol transport models show that the conversion rate from SO_2 to sulfate is about 76% [*Takemura et al.*, 2000] and about 36% of the converted sulfate is produced through the gas-phase reaction under the clear sky condition, which is our satellite measurement condition [*Chin et al.*, 2000].

4. Conclusions

[12] We have developed a four-channel algorithm to classify aerosols into four types of soil dust, carbonaceous, sulfate, and sea salt aerosols. This algorithm has been applied to the SeaWiFS data during the APEX-E2/ACE-Asia in the period of March to May 2001. The retrieved results were found to be in better agreement with the ground-based measurement values than with the conventional two-channel method. It was found that the East China Sea region had complicated mixtures of different types of aerosols. We also detected the sulfate aerosol plumes from the Mt. Oyama volcano located on Miyakejima Island. The mass conversion rate of the sulfate aerosols was estimated to be 23% of the emitted SO_2 amount.

[13] **Acknowledgments.** The authors are grateful to the SeaWiFS project and Japan Marine Science and Technology Center for providing the near real-time SeaWiFS HRPT data. We would like to express our appreciation to the TOMS project and JMA for providing the TOMS data and objective analysis data. We are also thankful to JST/APEX project, especially Prof. T. Takamura of Chiba University and Dr. A. Uchiyama of JMA for providing us with the SKYNET skyradiometer data.

References

Bluth, G. J. S., S. D. Doiron, C. C. Schnetzler, A. J. Krueger, and L. S. Walter, Global tracking of the SO_2 clouds from the June, 1991 Mount Pinatubo eruptions, *Geophys. Res. Lett.*, *19*, 151–154, 1992.

Chin, M., R. B. Rood, S.-J. Lin, J.-F. Müller, and A. M. Thompson, Atmospheric sulfur cycle simulated in the global model GOCART: Model description and global properties, *J. Geophys. Res.*, *105*, 24,671–24,687, 2000.

Deuzé, J. L., M. Herman, P. Goloub, D. Tanré, and A. Marchand, Characterization of aerosols over ocean from POLDER-ADEOS-1, *Geophys. Res. Lett.*, *26*, 1421–1425, 1999.

Deuzé, J. L., F. M. Bréon, C. Devaux, P. Goloub, M. Herman, B. Lafrance, F. Maignan, A. Marchand, F. Nadal, G. Perry, and D. Tanré, Remote sensing of aerosols over land surfaces from POLDER-ADEOS-1 polarized measurements, *J. Geophys. Res.*, *106*, 4913–4926, 2001.

Dubovik, O., A. Smirnov, B. N. Holben, M. D. King, Y. J. Kaufman, T. F. Eck, and I. Slutsker, Accuracy assessments of aerosol optical properties retrieved from Aerosol Robotic Network (AERONET) Sun and sky radiance measurements, *J. Geophys. Res.*, *105*, 9791–9806, 2000.

Herman, J. R., P. K. Bhartia, O. Torres, C. Hsu, C. Seftor, and E. Celarier, Global distribution of UV-absorbing aerosols from Nimbus 7/TOMS data, *J. Geophys. Res.*, *102*, 16,911–16,922, 1997.

Higurashi, A., and T. Nakajima, Development of a two channel aerosol retrieval algorithm on global scale using NOAA AVHRR, *J. Atmos. Sci.*, *56*, 924–941, 1999.

Higurashi, A., T. Nakajima, B. N. Holben, A. Smirnov, R. Frouin, and B. Chatenet, A study of global aerosol optical climatology with two channel AVHRR remote sensing, *J. Climate*, *13*, 2011–2027, 2000.

IPCC (the Intergovernmental Panel on Climate Change), *Climate Change 2001: The Scientific Basis*, edited by J. T. Houghton, Y. Ding, D. J. Griggs, M. Noguer, P. J. van der Linden, and D. Xiaosu, 881 pp., Cambridge Univ. Press., Cambridge and New York, 2001.

Kinoshita, K., N. Iino, I. Uno, A. Mori, and J. Kohno, Day and night detection of volcanic cloud and aerosol by NOAA/AVHRR data, Proc. Intern. Symp. On the Atmos. Correction of Satellite Data and Its Application to Global Environment. Chiba, 37 pp., 1998.

Lacis, A. A., and M. I. Mishchenko, Climate forcing, climate sensitivity, and climate response: A radiative modeling perspective on atmospheric aerosols, in *Aerosol forcing of climate*, edited by R. J. Charlson and J. Heintzenberg, pp. 11–42, John Wiley and Sons, Chichester, 1995.

Mishchenko, M. K., I. V. Geogdzhayev, B. Cairns, W. B. Rossow, and A. A. Lacis, Aerosol retrievals over the ocean using channel 1 and 2 AVHRR data: A sensitivity analysis and preliminary results, *Applied Optics*, *38*, 7325–7341, 1999.

Nakajima, T., and A. Higurashi, A use of two-channel radiances for an aerosol characterization from space, *Geophys. Res. Lett.*, *25*, 3815–3818, 1998.

Prata, A. J., Observations of volcanic ash clouds in the 10–12 micron window using AVHRR/2 data, *Int. J. Remote Sensing*, *10*, 751–761, 1989.

Sokolik, I., A. Andronova, and T. C. Johnson, Complex refractive index of atmospheric dust aerosols, *Atmos. Environ*, *16*, 2495–2502, 1993.

Takemura, T., H. Okamoto, Y. Maruyama, A. Numaguti, A. Higurashi, and T. Nakajima, Global three-dimensional simulation of aerosol optical thickness distribution of various origins, *J. Geophys. Res.*, *105*, 17,853–17,873, 2000.

WCP-55, *Report of the experts meeting on aerosols and their climate effects*, edited by A. Deepack and H. E. Gerber, 107 pp., World Meteorological Organization, 1983.

Wen, S., and W. I. Rose, Retrieval of size and total masses of particles in volcanic clouds using AVHRR bands 4 and 5, *J. Geophys. Res.*, *99*, 5421–5431, 1994.

A. Higurashi, National Institute for Environmental Studies, Ibaraki, Japan.
T. Nakajima, Center for Climate System Research Center, The University of Tokyo, Tokyo, Japan.